Palaeogeography, Palaeoclimatology, Palaeoecology 600 (2022) 111055

Contents lists available at ScienceDirect

Palaeogeography, Palaeoclimatology, Palaeoecology

journal homepage: www.elsevier.com/locate/palaeo

Late Holocene mangrove dynamics of the Doce River delta, southeastern Brazil: Implications for the understanding of mangrove resilience to sea-level changes and channel dynamics

Fernando A. Borges da Silva [a], Marlon C. França [a,b,c,*], Marcelo C.L. Cohen [a], Luiz C.R. Pessenda [d], Francis E. Mayle [e], Neuza A. Fontes [a], Flávio L. Lorente [d], Antônio Álvaro Buso Junior [d], Marisa de C. Piccolo [d], José A. Bendassolli [d], Kita Macario [f], Nicholas Culligan [g]

[a] Graduate Program of Geology and Geochemistry, Federal University of Pará, Belém 66077-530, Brazil
[b] Federal Institute of Pará, Belém 66090-020, Brazil
[c] Federal Institute of Espírito Santo, Piúma 29285-000, Brazil
[d] Center for Nuclear Energy in Agriculture, University of São Paulo, Piracicaba 13400-000, Brazil
[e] University of Reading, United Kingdom
[f] LAC-UFF AMS Laboratory-Fluminense Federal University, Niteroi, Brazil
[g] Department of Oceanography and Coastal Sciences, College of the Coast and Environment, Louisiana State University, Baton Rouge, LA 70803, United States of America

ARTICLE INFO

Editor: Howard Falcon-Lang

Keywords:
Pollen
Sea-level
Stable isotopes
Transitional sediments
Wave-influenced

ABSTRACT

This work aims to understand mangrove resilience to changes in a wave-influenced delta in southeastern Brazil during the late Holocene using an integrated analysis of palynology, sedimentology, and geochemistry ($\delta^{13}C$, $\delta^{15}N$, C:N and C:S ratio), and radiocarbon dating on two sediment cores. The data indicated three mangrove succession phases: 1) an estuarine point bar/tidal flat occupied by a mixture of mangrove species (~2660 - ~ 2050 cal yr BP); 2) a tidal flat dominated by *Laguncularia* mangroves (~2050 - ~ 900 cal yr BP); and 3) tidal flats with *Laguncularia* mangroves upstream and establishment of *Rhizophora/Avicennia* mangrove at the river mouth (~900 cal yr BP until present). The geochemical results suggest a dominance of C_3 terrestrial plants with a mixture of C_4 plants and organic matter of marine/estuarine origin throughout the late Holocene. *Laguncularia* and *Rhizophora* trees were established since ~ 2660 cal yr BP as pioneers, followed thereafter by *Avicennia*. Currently, tidal flats upstream are occupied by mangroves mainly represented by *Laguncularia*. *Rhizophora/Avicennia* mangroves occur at the mouth of the river. The relative sea-level fall during the late Holocene, as well as the channel dynamics, caused the development of tidal flats and mangrove succession inland. The succession of *Rhizophora*, *Laguncularia,* and *Avicennia*, followed by the permanence of only *Laguncularia*, is likely related to the resilience of each mangrove genus to habitat disturbance (e.g., salinity and sediment grain size fractions) caused by sea-level changes and channel dynamics. Our results show that mangroves may be resilient to the effects of Atlantic sea-level fluctuations, but the floristic structure in the past is different from that of today.

1. Introduction

The global distribution of mangroves has changed throughout geological and human history (Monacci et al., 2009). Studies along the Brazilian littoral zone using multi-proxy data have indicated expansion and contraction of mangrove areas during the Holocene (Amaral et al., 2006; Pessenda et al., 2008; Cohen et al., 2009; Smith et al., 2011; França et al., 2012; Guimarães et al., 2012; França et al., 2013, 2016). This mangrove dynamic is due to the combination of sea-level changes (Angulo et al., 2008), tectonic activities (Rossetti et al., 2012), and variations in fluvial discharge related to climate changes (Bush and Colinvaux, 1990; Bush et al., 2007). Mangroves are affected by complex interactions between tidal flood frequency, sediment and nutrient supply, and porewater salinity of intertidal flats (Hutchings and Saenger,

* Corresponding author at: Federal Institute of Espírito Santo – Brazil, Rua Augusto Costa de Oliveira, 660, Centro, CEP 29285-000 Piúma (ES), Brazil.
E-mail address: marlon.franca@ifes.edu.br (M.C. França).

https://doi.org/10.1016/j.palaeo.2022.111055
Received 13 December 2021; Received in revised form 11 May 2022; Accepted 12 May 2022
Available online 19 May 2022

1987; Wolanski et al., 1990; Masselink and Gehrels, 2015). Mangrove species differ in their responses to local variations in environmental conditions (Tomlinson, 1986).

Regarding natural influences on deltaic systems, sea-level fluctuations have affected coastal ecosystems, such as mangroves, along the Brazilian littoral (Lara and Cohen, 2009; Cohen et al., 2012, 2015; Pessenda et al., 2012; França et al., 2014, 2016; Fontes et al., 2017) during the Holocene. Coastal wetlands have the ability to maintain stability with sea-level (Kirwan and Murray, 2007). Equilibrium models of coastal wetlands consider several feedbacks that allow the coastal wetlands to keep their locations relative to the tidal range (Cohen et al., 2005; McKee et al., 2007), where sediment vertical accretion increases according to a depth of tidal flood (French and Stoddart, 1992; Furukawa and Wolanski, 1996; Blasco et al., 1996; Cahoon and Lynch, 1997; Krauss et al., 2013), and availability of accommodation space (Boyd and Penland, 1981; Woodroffe, 2002; Job et al., 2021), which allows the wetland to keep pace with relative sea level (Cahoon et al., 2006).

Mangroves occur parallel to the coastline, with zonations characterized by species dominating tidal flats more exposed to marine influence. Other species occupy higher tidal flats as a response to the substrate physical-chemical characteristics (Snedaker, 1982; Hutchings and Saenger, 1987). For instance, several mangrove tree species reach an ideal development at salinities between 5 and 25‰ (Burchett et al., 1989; Ball and Pidsley, 1995; Suárez and Medina, 2005) and respond to coastal processes and sediment deposition (França et al., 2012). *Rhizophora mangle* dominates on unstable tidal flats exposed to direct tidal influence. By contrast, *Avicennia germinans* dominates the higher tidal flats subjected to higher porewater salinities, and *Laguncularia racemosa* is commonly found in less saline environments and sandy sediments (Hogarth, 2007). Therefore, mangroves occur along environmental gradients characterized by salinity, landforms, and sediment types, which reflect fluvio-marine dynamics (Thom, 1984; Woodroffe, 1992).

The Doce River delta, southeastern Brazil, is considered one of the largest wave-dominated deltas of Brazil (Suguio et al., 1980; Dominguez et al., 1981; Martin et al., 1996). The delta progradation occurred during the last 5000 cal yr BP according to the late Holocene marine regression. The delta development occurred by beach ridge progradation according to a relative sea-level fall during the middle and late Holocene (Angulo et al., 2006; Cohen et al., 2020; de Toniolo et al., 2020). Thus, a relative sea-level fall may cause a seaward mangrove migration due to changes in flow energy and tidal inundation frequency (Cohen and Lara, 2003).

Mangroves expanded upstream of the Doce River delta, during the early-middle Holocene, followed by contraction and eventual disappearance of this ecosystem during the late Holocene (Buso Junior et al., 2013; França et al., 2013). The edges of the estuaries and tidal creeks are occupied by species typical of mangrove forests (Bernini et al., 2006). However, those works did not directly show the dominant plants along the Doce River estuary during the late Holocene. Therefore, it remains unclear when the mangrove types began to grow and the meaning of mangrove type succession. Mangroves may be resilient to sea-level fluctuations, but few works provided evidence about the relationship between the mangrove type succession and stressors factors, such as sea-level changes.

Then, how does each mangrove type respond to changes in depositional environments, controlled by sea-level fluctuations and input of different sediment grain sizes? It is a subject still open for discussion. Therefore, to contribute to the discussion and understanding of the mangrove resilience to changes in a wave-influenced delta (Southeastern Brazil) during the late Holocene, this paper presents the integration of multi-proxy data with sedimentary facies, pollen, isotopes ($\delta^{13}C$, $\delta^{15}N$) and elemental analysis.

2. Modern settings

2.1. Study area and geological setting

The study sites are located between 40° 04′– 39° 40′ W and 18° 34′–19° 48′ S and are adjacent to two river mouths, the Barra Seca River (sediment core MBN) and the São Mateus River (sediment core LI-34; reviewed in this work; França et al., 2016), which are each part of the Doce River Delta, State of Espírito Santo, southeastern Brazil (Fig. 1). The Holocene sedimentary dynamic in the study area is mainly controlled by relative sea-level change (RSL), fluvial sediment supply, and longshore currents. The formation of a barrier island/lagoonal system began at about 7000 cal yr BP (Suguio et al., 1982; Martin et al., 1996, 2003).

The region is mainly represented by the Barreiras Formation formed by continental and transitional deposits, with many broad valleys (Martin et al., 1996; Rossetti et al., 2013). Four geomorphological units may be identified in the study area: (1) a mountainous province with Precambrian rocks; (2) a tableland area, comprising the Barreiras Formation, gently sloping toward the coast, composed of sandstones, conglomerates and mudstones – attributed to Neogene marine transgressions (Dominguez, 2009; Rossetti et al., 2013); (3) a coastal plain area, with fluvial, transitional and shallow marine sediments, accumulated during RSL changes (Martin and Suguio, 1992); and (4) an inner continental shelf area with surficial sediments composed mainly by fine to coarse sands and mud sediments.

2.2. Modern climate and oceanography

The study area is located in a warm and humid tropical climate, with annual precipitation ~1190 mm and temperature ranges between 20° and 26 °C (Buso Junior et al., 2013). Precipitation occurs mainly during the summer (November – January), while the winter is characterized by a dry season (May – September), regulated by the Intertropical Convergence Zone (ITCZ) and the position of the South Atlantic Convergence Zone (SACZ) (Carvalho et al., 2004). The study area is affected by the South Atlantic trade winds belt (NE-E-SE) under the influence of a local high-pressure cell and the episodic advance of the Atlantic Polar Front, causing SSE winds (Dominguez et al., 1992; Martin et al., 1998).

The coastal plain of the Doce River has a maximum width of about 40 km and length of about 150 km (Bittencourt et al., 2007). This region is influenced by the Atlantic Ocean with microtidal semidiurnal, ranging below 2 m. The tidal water salinity is between 9 and 34‰. The Doce River has a maximum and minimum outflow of ~1900 and ~ 400 m^3/s, while the São Mateus River has a discharge ~11 m^3/s (Bernini et al., 2006).

2.3. Modern vegetation

Most of the study area is occupied by mangrove trees, ~5–10 m tall, represented by *R. mangle*, *L. racemosa,* and *A. germinans*. *Rhizophora* and *Laguncularia* trees occur mainly along the channels, while *A. germinans* grows mainly on higher tidal flats. Nowadays, mangrove forests are restricted to the northern sector of the Doce River Delta (Bernini et al., 2006), including the mouths of Barra Seca and São Mateus Rivers. The sandy coastal plain flora includes *Ipomoea pes-caprae*, *Hancornia speciosa*, *Chrysobalanus icaco*, *Hirtella americana, Cereus fernambucensis* and palm trees. It is also characterized by pioneering freshwater plants such as *Hypolytrum* sp., *Panicum* sp., and brackish water plants such as *Polygala cyparissias*, *Remiria maritima*, *Typha* sp., *Cyperus* sp., *Montrichardia* sp., *Tapirira guianensis*, and *Symphonia globulifera*. Herbaceous vegetation is also found at the coastal plain, represented by Araceae, Cyperaceae, and Poaceae. Tropical rainforest, occupying higher ground further inland, is predominantly characterized by the following families: Annonaceae, Fabaceae, Myrtaceae, Sapotaceae, Bignoniaceae, Lauraceae,

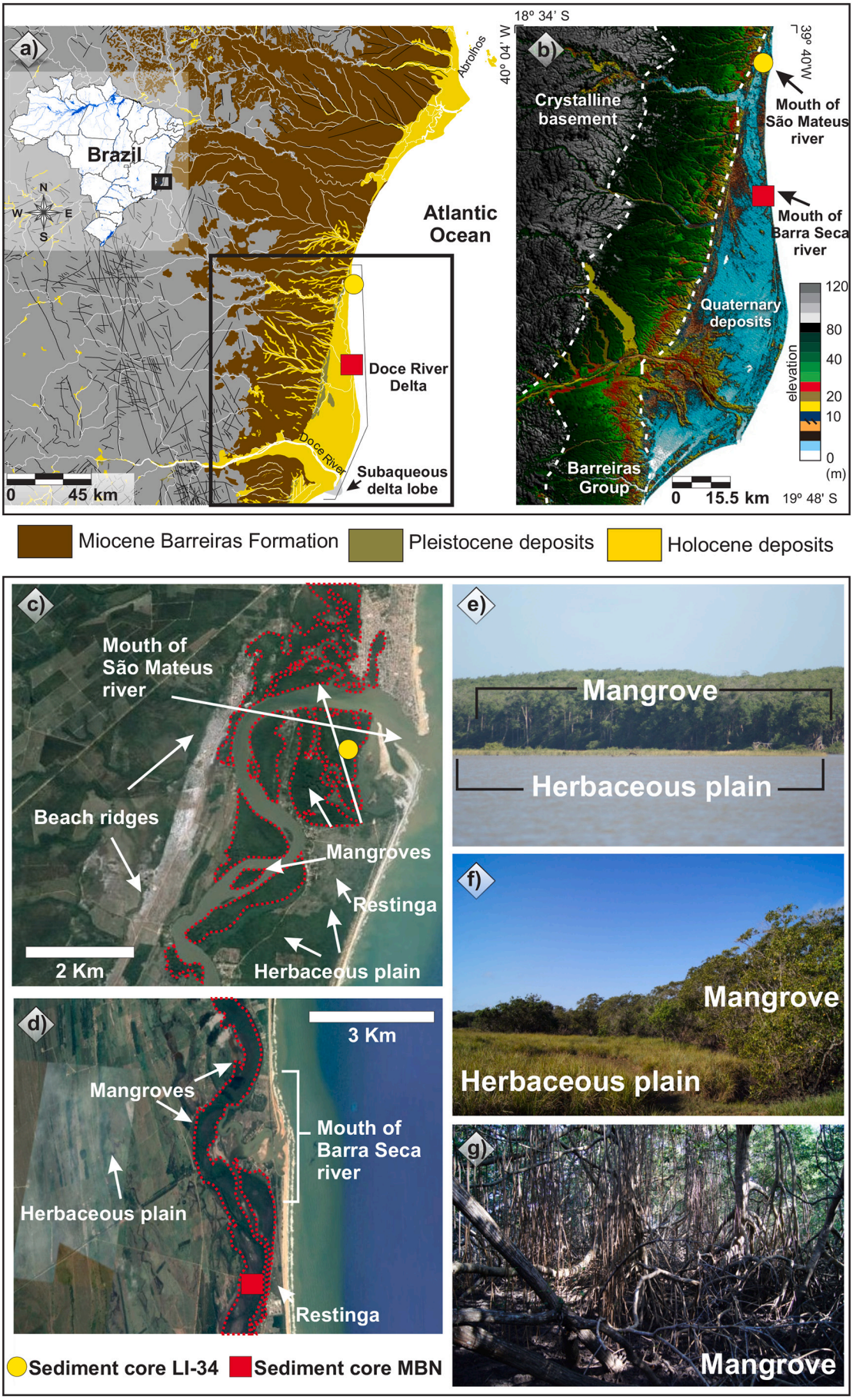

(caption on next page)

Fig. 1. Study area: a) Barreiras Formation, and Pleistocene and Holocene deposits under the influence of the Doce River Delta; b) topographic profile showing the differences between the topographic elevations of the Quaternary deposits, Barreiras Group, and crystalline basement; c) LI-34 core location showing geomorphological features such as beach ridges, herbaceous plain, and mangrove vegetation developed in the Holocene (Google Earth); d) MBN core location, showing herbaceous plain and mangroves developed in the Holocene (Google Earth); e) the contact between mangrove and herbaceous vegetation in the São Mateus River mouth; f) the contact between mangrove and herbaceous vegetation in the Barra Seca River mouth; g) mangrove vegetation composed mainly by *Rhizophora* and *Laguncularia* in the MBN area.

Hippocrateaceae, Euphorbiaceae, and Apocynaceae (Peixoto and Gentry, 1990).

3. Materials and methods

3.1. Fieldwork and sampling processing

For the description of the geological characteristics, the SPRING 3.6.03 processing system was used, which generated an image of composition RGB 543, elaborated from a LANDSAT 7 image, obtained in July 2011 from the Brazilian National Research Institute (INPE). Global Mapper 12 software was used to generate the topographic map, based on SRTM-90 data (http://srtm.usgs.gov/data/obtainingdata.html).

The sediment cores MBN (4.95 m depth, S 18°58′31.3″ / W 039°44′36.0″ and 0.6 m elevation – Barra Nova estuary) and LI-34 (4 m depth, S 18°36′27.4″/ W 39°44′40.4″ and 1 m elevation – São Mateus estuary) were retrieved from a mangrove muddy tidal flat (Fig. 1) using a Russian Peat sampler (USEPA, 1999). This area is a southeastern wave-dominated coast and has micro-tidal influence (Dominguez, 2009). Mean spring tidal range is 1.7 m in the area. The geographical positions of the cores were determined by GPS (Reference Datum: SAD69).

3.2. Radiocarbon dating

Based on stratigraphic discontinuities, suggested by color, lithology, and texture, seven bulk samples (10 g each) were chosen for radiocarbon analysis. The sediments were verified and physically cleaned under a stereomicroscope. Samples were placed in 2% HCl at 60 °C for 4 h to eliminate adsorbed carbonates. These samples were also rinsed and dried at 50 °C, following procedures described in Pessenda et al. (2012). The chronological context for the studied stratigraphic sequence was supplied by an accelerator mass spectrometer (AMS) radiocarbon dating at the ^{14}C Laboratory of Fluminense Federal University (LACUFF) and at UGAMS (University of Georgia – Center for Applied Isotope Studies). Radiocarbon ages were normalized to a δ^{13}C of −25‰ VPDB and reported as calibrated years (cal yr BP) (2σ) using CALIB 7.1 (Stuiver et al., 2018 - http://calib.org – accessed 2019-5-27). The dates (Table 1) are presented in the text as the median of the range of calibrated ages based on IntCal13 (Reimer et al., 2013).

3.3. Facies description

The cores were X-rayed to identify sedimentary structures and transported to the Laboratory of Chemical Oceanography/UFPA. The sediment grain size distribution was determined by laser diffraction using a Laser Particle Size SHIMADZU SALD 2101. The sediment grain size was based on the Wentworth (1922) with sand (2–0.0625 μm), silt (62.5–3.9 μm), and clay fractions (3.9–0.12 μm). Facies analysis involved description of color (Munsell Color, 2009), lithology, texture, and structure (Harper, 1984; Walker and James, 1992). The sedimentary facies codes followed Miall (1978).

3.4. Palynological analysis

Sediment samples (1.0 cm^3) were taken at 10 cm intervals and processed by standard pollen analytical techniques (Faegri and Inversen, 1989). This sampling interval along cores with 4–5 m long sampled from tidal flats with sedimentation rates between 1 and 20 mm/yr is appropriate for a palaeoenvironmental reconstruction during the late Holocene (Behling et al., 2004; Cohen et al., 2012; França et al., 2013). Pollen and spores were categorized according to the reference collections of about 4000 Brazilian flora taxa (Salgado-Labouriau, 1973; Markgraf and D'Antoni, 1978; Roubik and Moreno, 1991; Colinvaux et al., 1999) jointly with the reference collection of the Laboratory of Coastal Dynamics – Federal University of Pará and ^{14}C Laboratory of the Center for Nuclear Energy in Agriculture (CENA/USP). At least 300 terrestrial pollen grains were counted for each sample. The total terrestrial pollen sum excludes fern spores and aquatic pollen. Results were expressed as percentages of the total terrestrial pollen sum. The classification pollen taxa were based on pollen source: mangroves, trees and shrubs, palms, and herbs pollen. TILIA and TILIAGRAPH was used for calculations and graphical plotting (Grimm, 1990). The cluster analysis of pollen taxa was developed by CONISS (Grimm, 1987).

3.5. Isotopic and chemical analysis

Sediment samples (6–50 mg) were obtained along the cores at 10 cm intervals, and 2% HCl was used to remove carbonate. It was washed with distilled water until the pH reached 6, and dried at 50 °C. The sediment samples were analyzed for total organic carbon, nitrogen, and sulfur at the Stable Isotopes Laboratory and at the Nutrient Cycling Laboratory of the Center for Nuclear Energy in Agriculture (CENA/USP). Samples were analyzed in an ANCA SL2020 mass spectrometer and Sulfur Analyzer SC 144DR-LECO, respectively. The values are represented as a percentage of dry weight, with an analytical precision of 0.09% (TOC) and 0.07% (TN), respectively. The standard for sulfur analysis was

Table 1
Sediment samples selected C-14 dating and results from MBN and LI-34 core (Doce River Delta) with cody site, laboratory number, depth, material, ages ^{14}C yr BP conventional, calibrated and median (using Calib 6.0; Reimer et al., 2013).

Core	Cody site and laboratory number	Depth (m)	Material	Ages (^{14}C yr BP, 1σ)	Ages (cal yr BP, 2σ deviation)	Median of age range (cal yr BP)	Reference
LI-34	LACUFF13021	0.60–0.64	Bulk sed.	338 ± 43	307–409	360	França et al., 2016
LI-34	LACUFF13022	1.35–1.40	Bulk sed.	195 ± 37	105–114	110	França et al., 2016
LI-34	UGAMS15848	2.60–2.63	Bulk sed.	1200 ± 25	1210–1227	1220	França et al., 2016
LI-34	UGAMS15849	3.72–3.75	Bulk sed.	1440 ± 25	1299–1375	1340	França et al., 2016
MBN	UGAMS21210	0.97–0.99	Bulk sed.	2160 ± 20	2067–2081	2075	This work
MBN	UGAMS21211	3.80–3.82	Bulk sed.	2300 ± 20	2214–2216	2215	This work
MBN	UGAMS21212	4.77–4.79	Bulk sed.	2500 ± 20	2659–2664	2660	This work

0.031% (dry soil), from 0.028 to 0.034% (mean values). The ^{13}C and ^{15}N results are expressed as $\delta^{13}C$ and $\delta^{15}N$ with respect to VPDB standard and atmospheric air. Analytical precision is ±0.2‰ (Pessenda et al., 2004). In order to describe and understand the source of organic matter, the binary analyses between $\delta^{13}C$ vs. C:N (Meyers, 2003; Wilson et al., 2005; Lamb et al., 2006) and $\delta^{15}N$ vs. $\delta^{13}C$ (Peterson and Howarth, 1987; Fellerhoff et al., 2003) were used. Leaves of the vegetation units were sampled for isotopic $\delta^{13}C$ determination.

4. Results

4.1. Radiocarbon dating

The data presented in Table 1 provide late Holocene chronological control since ~2660 cal yr BP (core MBN, 4.79–4.77 m depth). The ^{14}C dates revealed that studied sediments were deposited according to a vertical accretion range between 0.45 and 20.07 mm/yr typical for the studied coast (16–1 mm/yr) during the mid-late Holocene. The high sedimentation rates have been attributed to a higher sediment accommodation space during the mid-late Holocene, caused by the middle Holocene high sea-level stand (Breithaupt et al., 2012, 2018; França et al., 2013, 2015, 2016; Lorente et al., 2014; Cohen et al., 2020). In this work we have used the informal terms mid and late Holocene instead of Middle or Late Holocene. The Quaternary literature has used variable informal usage of 'early', 'middle' or 'mid', and 'late' with the beginning of the middle Holocene ranges in age from 8 to 6 ka BP, while the end of the middle Holocene varies between 5 and 2.5 ka BP (e.g. Hoguin and Restifo, 2012). Walker et al. (2012) proposed an Early–Middle Holocene boundary at 8200 a BP and a Middle–Late Holocene boundary at 4200 a BP. However, proposal for relative sea-level changes for the Brazilian coast have used an informal scale for the Holocene (Angulo et al., 2006, 2016). Therefore, to discuss the temporal correlations of the events identified in this work with the relative sea-level changes proposed for the Brazilian coast, we decided to keep the Holocene informal scale for this work.

4.2. $\delta^{13}C$ values of modern vegetation

Thirty-two species of the most abundant plants were collected at the study sites. The $\delta^{13}C$ values range between −30.10‰ and − 11.48‰, indicating dominance of C_3 plants (Table 2). C_4 plants are restricted to the Poaceae family (*Paspalum* sp. and *Sporobolus virginicus*). Some species were characterized as CAM (Ecophysiology of Crassulacean Acid Metabolism), such as Cactaceae (C. fernambucensis) and Clusiaceae (*Clusia nemorosa*).

Table 2
Species from the Doce River Delta and their $\delta^{13}C$ value.

Vegetation type	Division or Family	Species/genus	Growth form	$\delta^{13}C$ (VPDB)
Lake	Asparagaceae	Unidentified	Herb	−26.03
	Cannaceae	*Canna glauca*	Herb	−26.55
	Cyperaceae	*Eleocharis*	Herb	−27.08
	Fabaceae	*Dalbergia ecastaphyllum*	Shrub	−28.71
		Senna sp.	Shrub	−29.31
	Malpighiaceae	*Stigmaphyllon ciliatum*	Liana	−27.57
	Nymphaeaceae	*Nymphaea ampla*	Herb	−28.52
	Poaceae	*Paspalum*	Herb	−11.48
		Unidentified	Herb	−12.56
	Typhaceae	*Typha domingensis*	Herb	−29.39
Mangrove	Combretaceae	*Laguncularia racemosa*	Tree	−27.39
		L. racemosa	Tree	−27.68
	Rhizophoraceae	*Rhizophora mangle*	Tree	−28.30
		R. mangle	Tree	−28.46
Restinga	Anacardiaceae	*Schinus terebinthifolia*	Shrub	−28.07
	Asteraceae	Unidentified	Herb	−26.42
	Boraginaceae	*Varronia curassavica*	Shrub	−30.10
	Cactaceae	*Cereus fernambucensis*	Shrub	−13.73
		C. fernambucensis	Shrub	−13.54
	Clusiaceae	*Clusia nemorosa*	Shrub	−15.42
		C. nemorosa	Shrub	−15.39
	Convolvulaceae	*Ipomoea imperati*	Herb	−24.74
		I. pes-caprae	Herb	−26.48
		I. pes-caprae	Herb	−26.53
	Fabaceae	*Stylosanthes guianensis*	Herb	−26.50
	Goodeniaceae	*Scaevela plumieri*	Shrub	−25.49
		S. plumieri	Shrub	−24.97
	Myrtaceae	*Eugenia vernicosa*	Tree	−30.15
		E. vernicosa	Tree	−29.99
	Nyctaginaceae	*Guapira pernambucensis*	Shrub	−27.45
	Poaceae	*Sporobolus virginicus*	Herb	−13.20
	Polygonaceae	*Coccoloba alnifolia*	Shrub	−28.04

4.3. Facies associations

The sediment cores were comprised of mostly greenish-gray or dark brown muddy and sandy silts (Figs. 2 and 3). The cores are characterized by massive sand (facies Sm), sand with cross-laminations (facies Sc), parallel lamination sand (facies Sp), lenticular (facies Hl), wavy (facies Hw), flaser (facies Hf) heterolithic bedding, and parallel laminated mud (facies Mp) with convolute lamination. Additionally, bioturbation structures, characterized by benthic tubes, plant remains, shells, roots, and root marks are present. Evaluation of sediment texture and structure and associated pollen and isotopic data ($\delta^{13}C$ and $\delta^{15}N$), together with C:N and C:S values, revealed three facies associations which represent a typical tidal flat setting, characterized by an estuarine point bar (facies association A), tidal flat with mangrove/herbs vegetation (facies association B), and estuarine channel (facies association C).

4.3.1. Facies association A (estuarine point bar)

The facies association A only occurs in core MBN between ~2660 and ~ 2215 cal yr BP (Fig. 2), between 4.9 and 3.8 m depth. It mainly consists of lenticular heterolithic bedding (facies Hl) with basal sand cross-lamination (facies Sc) and parallel sand lamination (facies Sp). Close to the top of this facies association inclined wavy (Hw) and flaser (Hf) heterolithic bedding with mud and organic matter deposition are present, which reflects point-bar lateral accretion within a meandering creek (Thomas et al., 1987).

The pollen record mainly shows an increase of herbaceous pollen (Fig. 4), between 2660 and 2215 cal yr BP (beginning of zone I), such as Poaceae (15–60%), Cyperaceae (5–15%), Asteraceae (2–4%), *Borreria* (<2%), and Convolvulaceae (<2%). Other ecological groups show a decreasing trend. Trees and shrubs are mainly characterized by Fabaceae (2–24%), Euphorbiaceae (5–15%), Rubiaceae (5–10%), Apocynaceae (3–7%), Moraceae (2–7%), *Mimosa* (2–5%), and *Alchornea* (~10%) pollen grains close to the top of this facies association. Palm pollen ranges between 5% and 16%. Mangrove pollen ranges between 5% and 16% abundance, mainly characterized by *Rhizophora* (3–6%), *Laguncularia* (5–16%), and *Avicennia* (<5%).

The $\delta^{13}C$ and C:N values oscillate between −27‰ and − 17‰ ($\bar{x}$ = −23‰), and 12 and 45 ($\bar{x}$ = 27.5) between 4.9 and 3.8 m depth, respectively (Fig. 2). $\delta^{15}N$ values range between 2.8‰ and 9.3‰ ($\bar{x}$ = 6.2‰) and the C:S ratio ranges between 0.38 and 5.18 ($\bar{x}$ = 2).

4.3.2. Facies association B (tidal flat with mangrove/herbs vegetation)

This association was identified in core MBN from 3.7 m depth to the surface (~2215 cal yr BP; Fig. 2) and LI-34 from 3.7 m depth to the surface (~1340 cal yr BP; Fig. 3). The facies association B is largely comprised of mud with fine and very fine sand, lenticular heterolothic

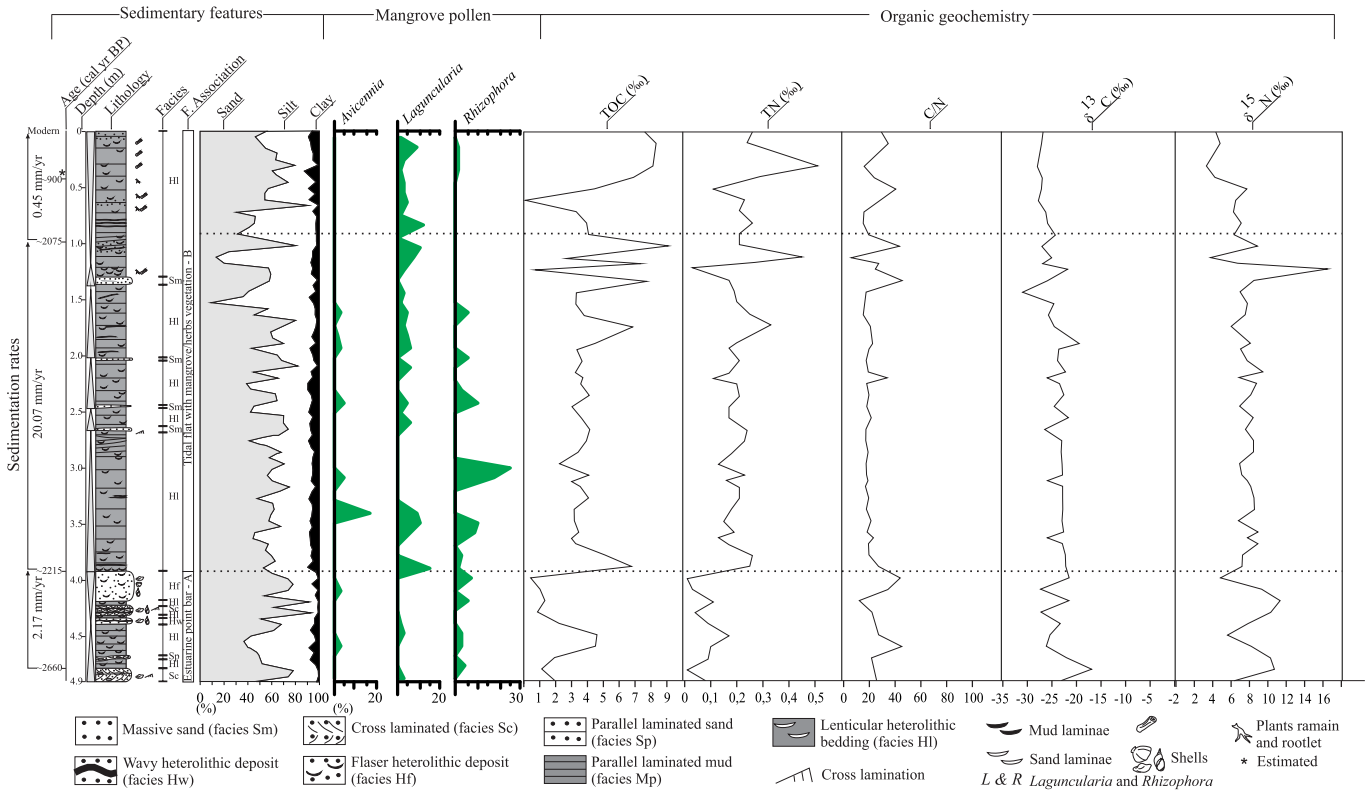

Fig. 2. Summary of the MBN sediment core, showing sedimentary features, ^{14}C dating, pollen data, and geochemical results.

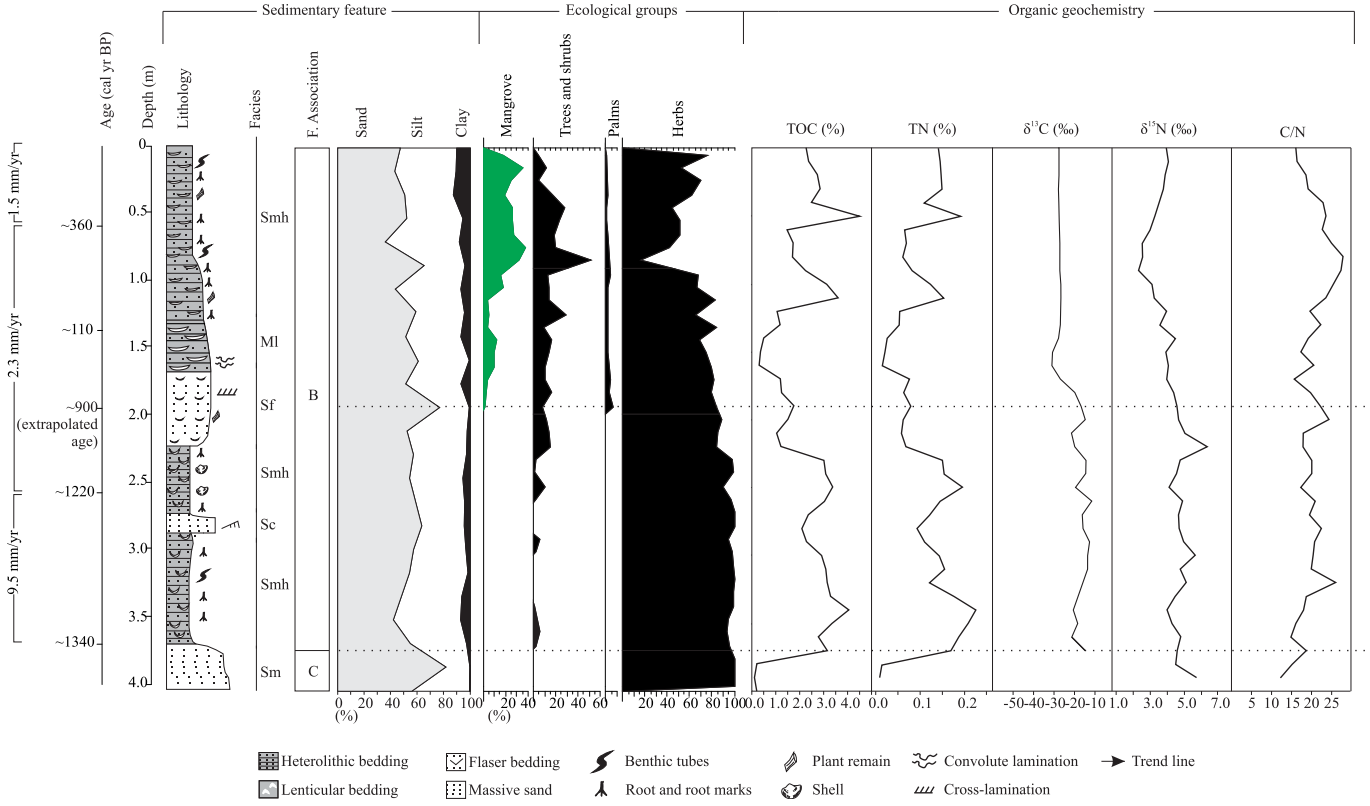

Fig. 3. Summary of the LI-34 sediment core, showing sedimentary features, ^{14}C dating, pollen data, and geochemical results.

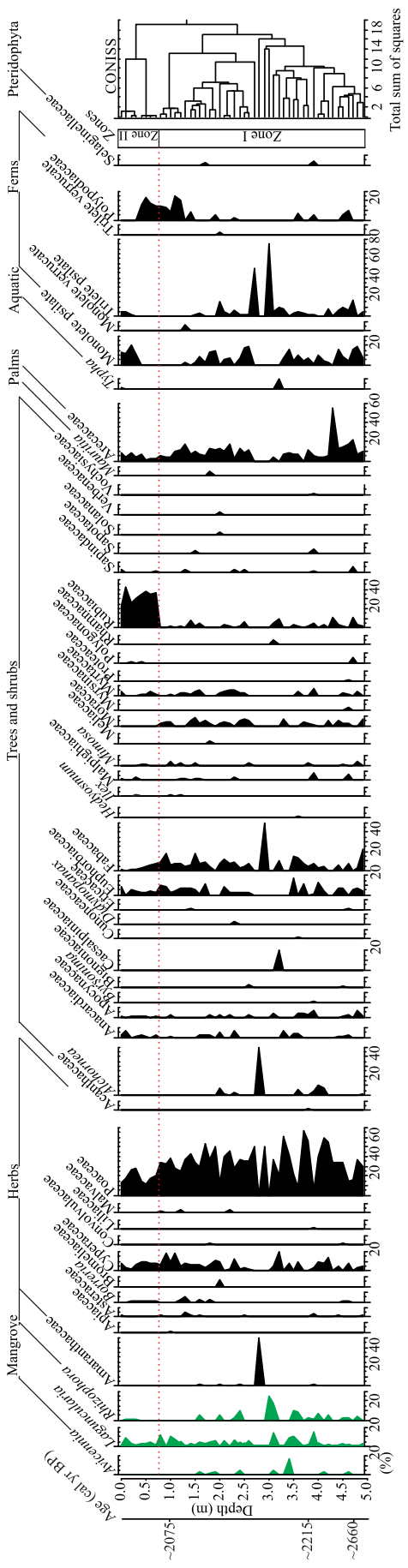

Fig. 4. Pollen diagram record for core MBN. Ecological group abundance is shown in percentage of total pollen sum. Phase boundaries are marked by the red dotted lines. (For interpretation of the references to color in this figure legend, the reader is referred to the web version of this article.)

bedding (facies Hl), massive sand deposits (facies Sm), flaser bedding (facies Sf), cross-lamination sand (facies Sc), and parallel laminated mud bedding (facies SMh). This deposit also contains benthic tubes, shells fragments, root, and root marks.

The pollen assemblage of facies association B is mainly characterized by herbaceous pollen, but trees, shrubs, palms, and mangrove pollen are also present (Figs. 4 and 5). The herbaceous pollen is mainly characterized by Poaceae (7–70%), Cyperaceae (4–30%), Amaranthaceae (2–50%), *Borreria* (1–14%), Asteraceae (3–11%), Malvaceae (1–5%), and *Smilax* (1–6%). The most common tree and shrub taxa are: *Alchornea* (5–50%), Fabaceae (2–50%), Rubiaceae (2–45%), Euphorbiaceae (5–20%), Moraceae (2–15%), *Mimosa* (2–8%), Malpighiaceae (5–7%), Apocynaceae (2–6%), *Cecropia* (2–6%), Myrtaceae (2–6%), and Anacardiaceae (2–5%), together with low percentage abundance (<5%) of *Croton*, Meliaceae, and Sapindaceae. Aquatic taxa consist of *Typha* (10%), and palms (Arecaceae) range from 2 to 55% abundance. Mangrove pollen assemblages are characterized by *Avicennia*, *Laguncularia,* and *Rhizophora* in core MBN (4–25%), and *Avicennia* and *Rhizophora* in core LI-34 (5–37%). In the core MBN a mangrove intra-species variation with the disappearance of *Avicennia* and *Rhizophora* occurred near 1.5 m, between ~2215 and ~ 2075 cal yr BP, while *Laguncularia* pollen was present to the surface. The surface-core pollen assemblage had low abundance of *Rhizophora* pollen (1–2%) (Fig. 4). In contrast, in core LI-34, *Rhizophora* pollen is present in the record since at least 900 yr BP (2.0 m), and *Avicennia* is present since 360 cal yr BP (1.5 m) (Fig. 5).

$\delta^{13}C$ values range between −31‰ and − 11.5‰ ($\bar{x}$ = −23.3‰), while $\delta^{15}N$ values range between 1.3‰ and 14.5‰ ($\bar{x}$ = 4.8‰). C:N ratios range between 5.96 and 45.5 ($\bar{x}$ = 20.8) and C:S ratios (MBN core) range between 0.02 and 3.65 ($\bar{x}$ = 2.05).

4.3.3. Facies association C (estuarine channel)

The facies association C was only identified at the base of core LI-34 (~1340 cal yr BP) (Figs. 3 and 5), between 4.0 and 3.7 m, which consists of a massive sand deposit (facies Sm) with fine to medium-grained sediments and shell fragments.

Pollen analysis indicated the predominance of herbaceous pollen (Fig. 5), such as Poaceae (44–56%), Cyperaceae (41–49%), Amaranthaceae (3–6%), Asteraceae, and *Borreria* (~2%) (Fig. 5). The $\delta^{13}C$ values vary between −31 and − 27‰. The $\delta^{15}N$ values oscillate between 4 and 6‰. The TOC and nitrogen values are relatively low at the bottom of the core (0.1–0.2% and ~ 0.01%, respectively). C:N ratios range between 12 and 15 (Fig. 3).

5. Interpretation and discussion

5.1. Paleoenvironmental reconstruction

The multi-proxy data reveal three environmental phases spanning the last ~2660 cal yr BP, based on changes in RSL and sediment supply (Fig. 6). The first phase, between ~2660 and ~ 2050 cal yr BP, is mainly marked by the presence of *Rhizophora, Laguncularia,* and *Avicennia* on point bar deposits inland (Figs. 2 and 6). The second phase, between ~2050 and ~ 900 cal yr BP, is marked by the disappearance of *Avicennia* and *Rhizophora* from the MBN site. During the last ~900 cal yr BP, the third phase is marked by extensive expansion of *Laguncularia* mangroves on tidal flats upriver and the presence of *Rhizophora* mangroves giving way to *Avicennia* mangroves at the mouth of the São Mateus River (core LI-34).

5.1.1. Phase 1 (~2660 to ~2050 cal yr BP)

This phase is marked by sand and mud massive sediments, followed by parallel laminated mud/sand with bioturbation structures. It is indicative of both high and low energy flow. These sedimentary features, together with the pollen and geochemical characteristics, suggest the development of a point bar and presence of herbaceous plants and mangrove trees, represented by *Avicennia, Laguncularia,* and *Rhizophora*

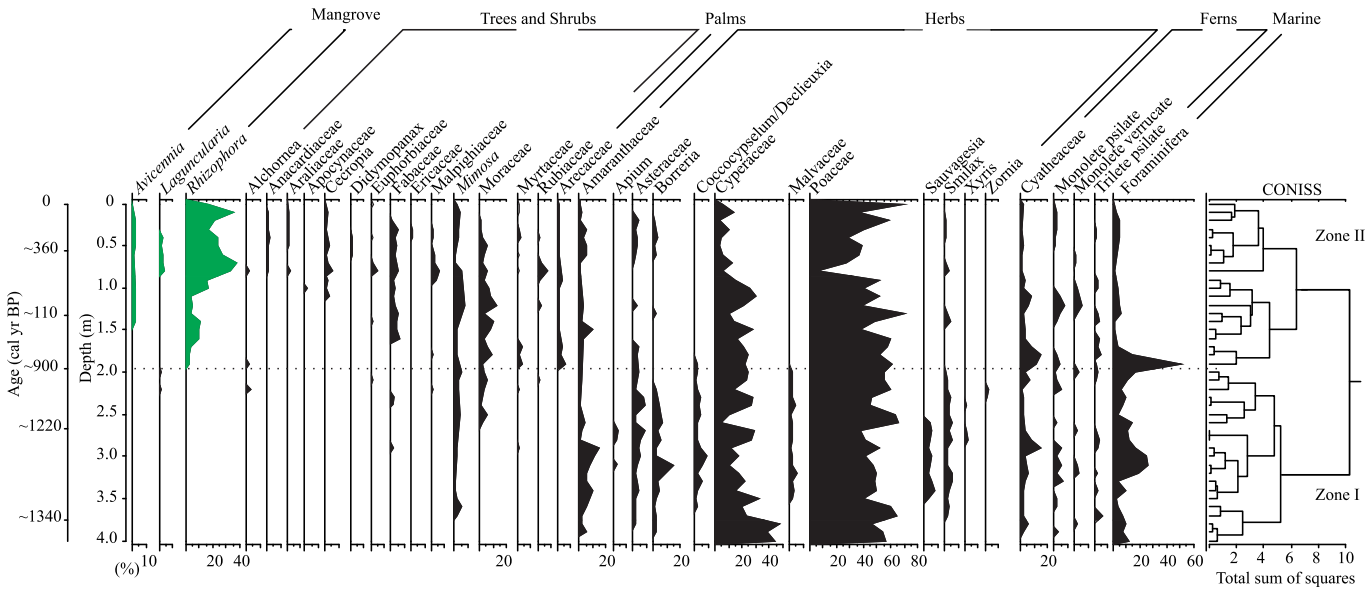

Fig. 5. Pollen diagram record for core LI-34. Ecological group abundance is shown in percentage of total pollen sum. Zone boundaries are marked by black dotted lines.

since at least ~2660 cal yr BP, behind the late Holocene beach ridges. During this phase there was a transition from a point bar to a tidal flat. The end of this phase is marked by the disappearance of *Avicennia* and *Rhizophora* mangrove taxa around 2075 cal yr BP, with only *Laguncularia* mangrove trees remaining. The latter was likely caused by channel migration and a decrease in sea-level, leading to an increase in erosion. Therefore, a common zonation from the intertidal fringe to higher elevations landward indicates the following genus mangrove gradient: *Rhizophora* > *Avicennia* > *Laguncularia* (Woodroffe, 1982). Furthermore, the decrease in *Rhizophora* and *Avicennia* trees, leaving only *Laguncularia* trees, which commonly occupy less saline environments (Hogarth, 2007), indicates a reduction in salinity, probably due to a sea-level drop and/or to the wet climate. In addition, *Laguncularia* trees have greater resilience to adverse conditions (Tomlinson, 1986; Gu et al., 2019; Cohen et al., 2020). We interpret this sequence of mangrove dynamics to signify relative sea-level fall over the last 5500 cal yr BP, which led to an increase in sediment supply (França et al., 2016). Locally, the establishment of mangroves depends on the dynamics of channel migration. The relationship between $\delta^{13}C$ values, ranging from −27 and − 16‰, and C:N ratios (12–45), indicates that sedimentary organic matter was sourced from mixing between C_3 terrestrial plants and marine dissolved organic carbon-DOC (Fig. 7), suggesting estuarine zones between ~2660 and ~ 2050 cal yr BP.

5.1.2. Phase 2 (~2050 to ~900 cal yr BP)

During this phase a mangrove succession developed, whereby the mangrove community of preceding phase 1, containing a mix of *Avicennia, Rhizophora*, and *Laguncularia* trees, was replaced by a monospecific mangrove community dominated by *Laguncularia* trees at the MBN site. Tidal flats constitute favorable hydrodynamic conditions for mangrove development due to muddy sedimentation, with low-energy waves and low current velocity. During this phase, oscillations in wave energy and velocity produced cross-lamination sand, inducing the migration of small sand ripples (Reineck and Singh, 1980). Furthermore, the upward fineing sequence indicates a decrease in energy flow, favouring the establishment of a tidal flat, with sedimentation rates around 20 mm/yr. These hydrodynamic conditions favored mangrove development.

During this phase $\delta^{13}C$ values ranging between −28 and − 22‰, together with C:N ratios between 6 and 40, indicate that organic matter was sourced predominantly from C_3 plants ($\delta^{13}C$: −32‰ to −21‰, C:*N* > 20; Deines, 1980) (Fig. 2, MBN core). An estuarine environment is consistent with $\delta^{13}C$ values ranging from −32‰ to −26‰, and C:N ratios from <25 to >6, according to Fig. 7 (Lamb et al., 2006). The $\delta^{15}N$ values between 4 and 7.4‰ ($\bar{x}$ = 5.8‰) suggest a mixture of terrestrial plants and aquatic organic matter (Sukigara and Saino, 2005). The trends of rising carbon and nitrogen values signify mangrove establishment.

5.1.3. Phase 3 (900 cal yr BP until present)

This phase is marked by the abundance of *Laguncularia* and *Rhizophora* trees occupying upriver tidal flats at the MBN site, as well as the presence of a mangrove ecosystem dominated by *Rhizophora* and *Avicennia, and some Laguncularia (<3%)*, on tidal flats near the mouth of the São Mateus River at the LI-34 site (Fig. 6). The sediments are characterized by heterolithic bedding and massive sand, with plant remains and rootlets. At the LI-34 site, near the São Mateus River mouth, this phase is marked by sand deposition, typical of the mouth of an estuarine channel. Following a sea level decrease, relative sea-level stabilized (Angulo et al., 2006). This favored mangrove establishment, characterized by *Rhizophora* and *Avicennia,* around 900 cal yr BP at the LI-34 site and mangrove migration to the mouth of the São Mateus River.

According to the $\delta^{13}C$ values (around −28‰), and C:N ratios (16–27), tidal flats close to the mouth of the Barra Seca and São Mateus River were characterized by C_3 terrestrial plants and a mixture of freshwater/estuarine dissolved organic carbon (DOC) (Fig. 7), consistent with a marine influence and mangrove colonization.

5.2. Floristic changes to mangrove communities

Mangroves expanded upstream of the Doce River delta, southeastern Brazil, during the early-middle Holocene, and were occupying topographically higher flats in the mid-Holocene (França et al., 2015). However, the RSL fall combined with the higher sediment fluvial discharge caused a coastal progradation over the last ~6350 cal yr (Buso Junior et al., 2013; França et al., 2013, 2016; Lorente et al., 2014). According to our data, mangroves migrated to lower tidal flats behind the current beach ridges between ~2660 and ~ 900 cal yr BP due to sea-level drop. The stabilization of relative sea-level during the last 900 cal yr BP contributed to the development of tidal flats and mangrove expansion, with a predominance of *Laguncularia* mangroves upstream and the establishment of *Rhizophora/Avicennia* mangroves at the mouth

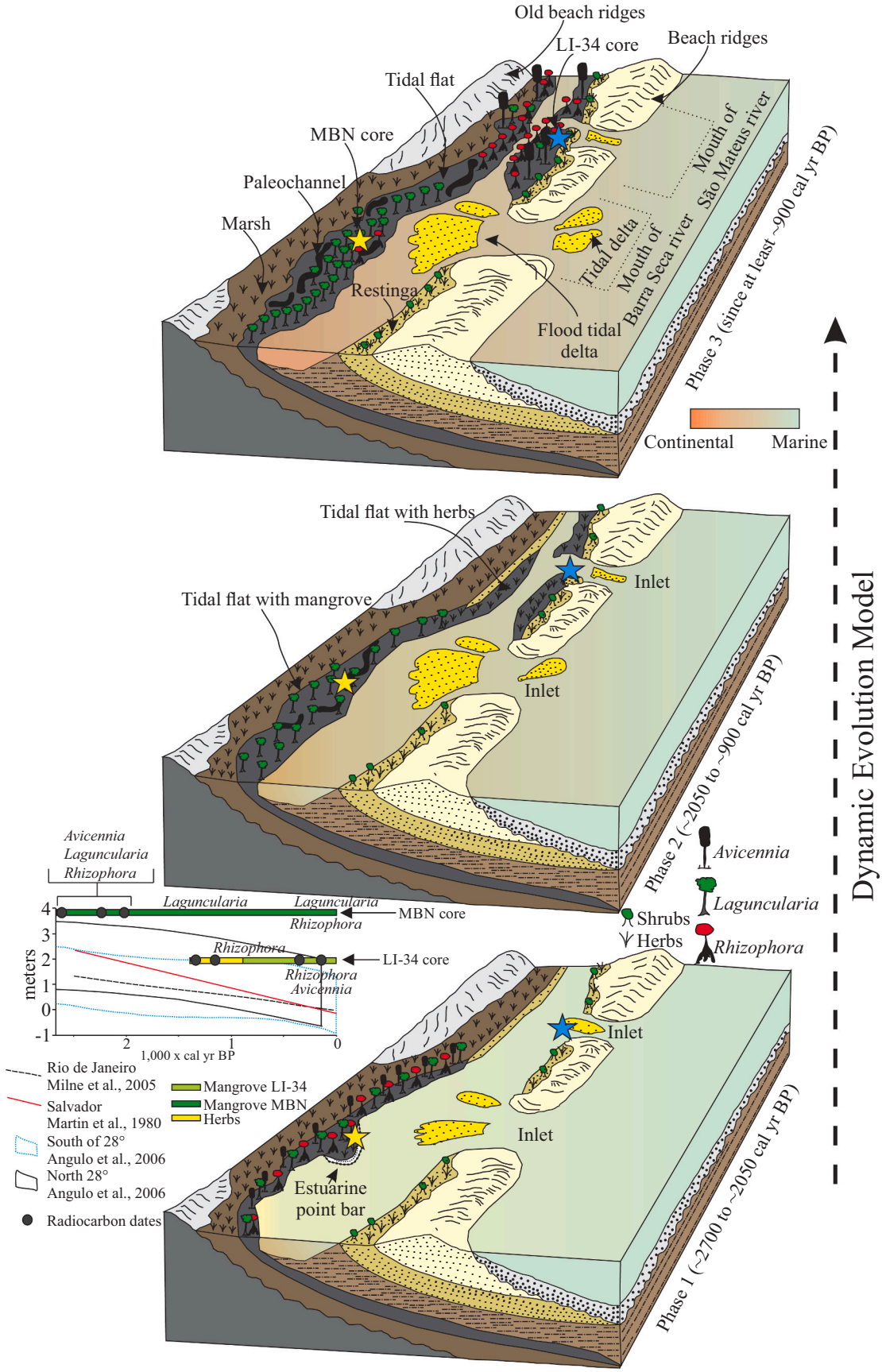

Fig. 6. Model of paleoenvironmental changes in the late Holocene. Sea level fall was expressed in the figure according to previous studies (Martin et al., 1980; Milne and Bassett, 2005; Angulo et al., 2006).

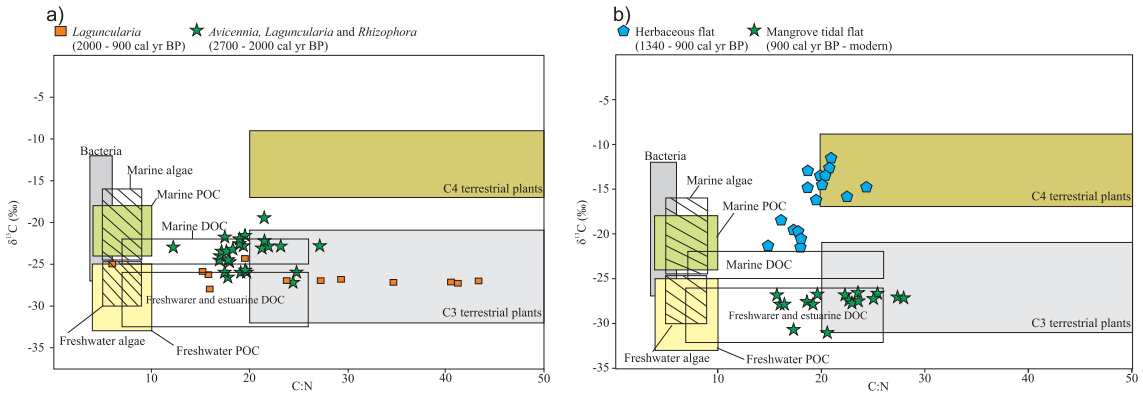

Fig. 7. Diagrams for core MBN (a) and core LI-34 (b) illustrating the relationship between $\delta^{13}C$ vs. C:N for the different coastal organic matter sources during the late Holocene in southeastern Brazil. Interpretation is according to data presented by Meyers (2003) and Lamb et al. (2006).

of the rivers.

Mangrove species differ in their responses to local environmental conditions, which directly affect their development (Tomlinson, 1986). These environmental variations may drive either positive or negative feedback, depending on the taxon. For example, salinity variations may impair the growth and reproduction of certain mangrove species, such as *Avicennia* (Naidoo et al., 2011). On the other hand, an increase in salinity can drive an increase in the production of chlorophyll-*a* and b in L. *racemosa* (Sobrado, 2000), giving it greater resistance to adverse conditions and increasing its colonization potential. It is important to emphasize that, unlike *Rhizophora*, both *Laguncularia* and *Avicennia* are adapted to hypersalinity conditions. However, for successful germination, *Laguncularia* can withstand longer periods of salinity than *Avicennia* (Cavalcanti et al., 2007), which means that *Laguncularia* is relatively better adapted for growth in the middle of the spatial-temporal salinity spectrum and, accordingly, has higher plasticity (Tomlinson, 1986). Furthermore, the increase in flow energy, evidenced by the deposition of sandy sediments, may also contribute to mangrove community changes, leading to species turnover (França et al., 2012). For example, *Laguncularia* is commonly found in more disturbed environments than those of *Rhizophora* and *Avicennia* (Hogarth, 2007), and may withstand the impact caused by disasters and/or human pollution, such as metal contamination at the Doce River estuary after the dam collapse on 5th November 2015 (Fernandes et al., 2016). On the sand bars, coastal dynamics caused high mangrove mortality by erosion or sand sedimentation on mangrove muddy substrates, which have caused tree roots to suffer from anoxia (Gil-Torres and Ulloa-Delgado, 2001). Mangroves dominated by *Rhizophora* retreated along the northern Brazilian coastline due to landward sand migration that covered the mudflat and asphyxiated vegetation (Cohen and Lara, 2003; França et al., 2012).

The ecophysiological characteristics of L. *racemosa* highlight its important role as a pioneer species in mangrove succession; e.g. creating suitable microclimatic conditions (raising humidity and reducing soil temperature) to facilitate colonization by other mangrove tree species (Cavalcanti et al., 2007). Thus, mangroves have demonstrated considerable resilience over timescales commensurate with shoreline evolution, resisting natural disturbances, and human impacts (Alongi, 2008).

Our multi-proxy late Holocene records show that, by the end of the first phase (2075 cal yr BP), populations of *Avicennia* and *Rhizophora* had decreased substantially, with only *Laguncularia* remaining in the area near the Barra Seca River mouth. We argue that these floristic changes were most likely caused by relative sea-level fall and channel migrations. These processes triggered successive changes in the salinity and grain size of the sedimentary environment, thus destabilizing the system. According to Kathiresan and Thangam (1990), fluctuations in the environment salinity have a more relevant effect on mangrove species than a constant hypersalinity. Once a mangrove forest is established, successive changes in salinity can lead to the death of adult individuals as they have less plasticity than seedlings. This effect was observed in situations where there were changes in the flood dynamics caused by changes in the mouth of a river (Tognella et al., 2006). Our sedimentary profiles show that our study area experienced high energy in several periods due to the presence of laminations of sand from the base toward the top of the core, suggesting signifying fluctuations in the environment salinity. These variations would have driven the disappearance of the genera *Avicennia* and *Rhizophora* from the region near the Barra Seca River mouth. In contrast, the pioneer tree *Laguncularia* would have been resilient to these salinity variations. In the upper part of the MBN core (phase 3), no sandy deposition pulses were observed, thus indicating a possible stabilization in the system, which together with the decrease in RSL and greater continental influence, decreased the salinity of the environment and allowed the reappearance of individuals of *Rhizophora*.

6. Conclusions

This paper's multi-proxy data reveal the mangrove response to the relative sea-level fall and sedimentary dynamics of the Doce River Delta region of Espírito Santo state, southeastern Brazil in the late Holocene. Our results show that the mangrove may be resilient to Atlantic sea-level fluctuations, but that the previous floristic composition of the mangrove vegetation differed from what is currently present. Therefore, this study resolves a key research question of widespread interest, revealing the mangrove response to the sediment dynamics and sea-level fluctuations. Thus, mangrove ecosystems have existed in the current coastal zone since at least ~2660 cal yr BP, with a dynamic history which comprises three phases: 1°) an estuarine point bar/tidal flat with mixed mangroves (~2660 until ~ 2050 cal yr BP), 2°) a tidal flat with *Laguncularia* mangroves (~2050 until ~ 900 cal yr BP), and 3°) tidal flats with *Laguncularia* mangroves upstream and establishment of *Rhizophora/Avicennia* mangroves at the mouth of the rivers (~900 cal yr BP until present). The geochemical results indicate a dominance of C_3 terrestrial plants with some influence of C_4 plants and organic matter of marine/estuarine origin along the studied cores. The pollen data show that the mangroves in this region have been present since at least ~ 2660 cal yr BP. *Laguncularia* and *Rhizophora* trees were the initial pioneers in mangrove development, followed by *Avicennia*. Currently, mangroves in the MBN area (Barra Nova estuary) are dominated by *Laguncularia*. *Rhizophora/Avicennia* mangroves occur at the mouth of the rivers. Therefore, our data reveal changes in the mangrove ecosystem due to a gradual relative sea-level fall during the late Holocene and the sedimentary dynamics which resulted in the development of tidal flats and a mangrove succession. The succession from a mixed mangrove community (*Rhizophora*, *Laguncularia*, and *Avicennia*) to a monospecific mangrove community comprised only of *Laguncularia* is likely due to differing tolerances of these taxa to variations in salinity, sediment deposition associated with changes in sea-level and channel dynamics,

and immediate impact caused by disasters and/or human pollution.

Declaration of Competing Interest

The authors declare that they have no known competing financial interests or personal relationships that could have appeared to influence the work reported in this paper.

Acknowledgments

We would like to thank the members of the Laboratory of Coastal Dynamics (LADIC-UFPA), Center for Nuclear Energy in Agriculture (CENA-USP), Vale Natural Reserve (Linhares, ES) and the students from Laboratory of Chemical-Oceanography (UFPA) for their support. This study was financed by FAPESP (03615-5/2007 and 00995-7/11), FAPES (093/2020, 03/2021, 441/2021, and 282/2021) and in part by the Coordenação de Aperfeiçoamento de Pessoal de Nível Superior - Brasil (CAPES) - Finance Code 001. The second author would like to thank CNPq for research scholarship (305074/2017-2 and 309618/2020-7). We also wish to thank Geovani S. Siqueira for the help with the preparation of plant specimens.

References

Alongi, D., 2008. Mangrove forests: Resilience, protection from tsunamis, and responses to global climate change. Estuarine Costal Shelf Sci. 76 (1), 1–13.
Amaral, P.G.C., Ledru, M.P., Branco, F.R., Giannini, P.C.F., 2006. Late Holocene development of a mangrove ecosystem in southeastern Brazil (Itanhaém, state of São Paulo). Palaeogeogr. Palaeoclimatol. Palaeoecol. 241 (3), 608–620.
Angulo, R.J., Lessa, G.C., Souza, M.C., 2006. A critical review of Mid- to Late-Holocene Sea-level fluctuations on the eastern Brazilian coastline. Quat. Sci. Rev. 25, 486–506.
Angulo, R.J., De Souza, M.C., Assine, M.L., Pessenda, L.C.R., Disaró, S.T., 2008. Chronostratigraphy and radiocarbon age inversion in the Holocene regressive barrier of Paraná, southern Brazil. Mar. Geol. 252, 111–119.
Angulo, R.J., Giannini, P.C.F., De Souza, M.C., Lessa, G.C., Angulo, R.J., Giannini, P.C.F., De Souza, M.C., Lessa, G.C., 2016. Holocene paleo-sea level changes along the coast of Rio de Janeiro, southern Brazil: comment on Castro et al. (2014). An. Acad. Bras. Cienc. 88, 2105–2111.
Ball, M.C., Pidsley, S.M., 1995. Growth responses to salinity in relation to distribution of two mangrove species, *Sonneratia alba* and *S. lanceolata*, in northern Australia. Funct. Ecol. 9, 77–85.
Behling, H., Cohen, M.L., Lara, R., 2004. Late Holocene mangrove dynamics of Marajó Island in Amazonia, northern Brazil. Vegetat. Hist. Archaeobot. 13, 73–80.
Bernini, E.S.M.A., Carmo, T.M., Cuzzuol, G.R.F., 2006. Composição química do sedimento e de folhas das espécies do manguezal do estuário do rio São Mateus, Espírito Santo, Brasil. Rev. Bras. Bot. 29, 686–699.
Bittencourt, A.C.S.P., Dominguez, J.M.L., Martin, L., Silva, I.R., De-Medeiros, K.O.P., 2007. Past and current sediment dispersion pattern estimates through numerical modeling of wave climate: an example of the Holocene delta of the Doce River, Espírito Santo, Brazil. An. Acad. Bras. Cienc. 79, 333–341.
Blasco, F., Saenger, P., Janodet, E., 1996. Mangrove as indicators of coastal change. Catena 27, 167–178.
Boyd, R., Penland, S., 1981. Washover of deltaic barriers on the Lousiana coast. Trans. Gulf Coast Assoc. Geol. Soc. 31, 243–248.
Breithaupt, J., Smoak, J., Smith, T., Sanders, C., Hoare, A., 2012. Organic carbon burial rates in mangrove sediments: Strengthening the global budget. Glob. Biogeochem. Cycles 26 (3), 1–11.
Breithaupt, J., Smoak, J., Byrne, R., Waters, M., Moyer, R., Sanders, C., 2018. Avoiding timescale bias in assessments of coastal wetland vertical change. Limnol. Oceanogr. 63 (S1), 477–495.
Burchett, M.D., Clarke, C.J., Field, C.D., Pulkownik, A., 1989. Growth and respiration in two mangrove species at a ranges of salinities. Physiol. Plant. 75, 299–303.
Bush, M.B., Colinvaux, P.A., 1990. A long record of climatic and vegetation change in lowland Panamá. J. Veget. Sci. Uppsala 1, 105–118.
Bush, A.M., Bambach, R.K., Daley, G.M., 2007. Changes in theoretical ecospace utilization in marine fossil assemblages between the mid-Paleozoic and late Cenozoic. Paleobiol. 33, 76–97.
Buso Junior, A.A., Pessenda, L.C.R., Oliveira, P.E.O., Giannini, P.C.F., Cohen, M.C.L., Ribeiro, C.V., Oliveira, S.M.B., Favaro, D.I.T., Rossetti, D.F., Lorente, F.L., Borotti Filho, M.A., Schiavo, J.A., Bendassolli, J.A., França, M.C., Guimaraes, J.T.F., Siqueira, G.S., 2013. Late Pleistocene and Holocene vegetation, climate dynamics, and Amazonian taxa in the Atlantic Rainforest of Linhares, Southeastern Brazil. Radiocarb. 55, 1747–1762.
Cahoon, D.R., Lynch, J.C., 1997. Vertical accretion and shallow subsidence in a mangrove forest of southwestern Florida, U.S.A. Mangrove Salt Marshes 1, 173–186.
Cahoon, D.R., Hensel, P.F., Spencer, T., Reed, D.J., McKee, K.L., Saintilan, N., 2006. Coastal wetland vulnerability to relative sea-level rise: wetland elevation trends and process controls. Wetlands Nat. Resour. Manag. 190, 271–292.
Carvalho, L.M.V., Jones, C., Liebmann, B., 2004. The South Atlantic convergence zone: Intensity, form, persistence, and relationships with intraseasonal to interannual activity and extreme rainfall. J. Clim. 17, 88–108.
Cavalcanti, V.F., Andrade, A.C.S., Soares, M.L.G., 2007. Germination of *Avicennia schaueriana* and *Laguncularia racemosa* from two physiographic types of mangrove forest. Aquat. Bot. 86 (3), 285–290.
Cohen, M.C.L., Lara, R.J., 2003. Temporal changes of mangrove vegetation boundaries in Amazônia: application of GIS and remote sensing techniques. Wetl. Ecol. Manag. 11, 223–231.
Cohen, M.C.L., Souza Filho, P.W., Lara, R.L., Behling, H., Angulo, R., 2005. A model of Holocene mangrove development and relative sea-level changes on the Bragança Peninsula (northern Brazil). Wetl. Ecol. Manag. 13, 433–443.
Cohen, M.C.L., Behling, H., Lara, R.J., Smith, C.B., Matos, H.R.S., Vedel, V., 2009. Impact of sea-level and climatic changes on the Amazon coastal wetlands during the late Holocene. Veg. Hist. Archaeobotany 10–20.
Cohen, M.C.L., Pessenda, L.C.R., Behling, H., Rossetti, D.F., França, M.C., Guimarães, J.T. F., Friaes, Y.S., Smith, C.B., 2012. Holocene palaeoenvironmental history of the Amazonian mangrove belt. Quat. Sci. Rev. 55, 50–58.
Cohen, M.L., Alves, I.C.C., França, M.C., Pessenda, L.C.R., Rossetti, D.F., 2015. Relative Sea-level and climatic changes in the Amazon littoral during the last 500 years. Catena 133, 441–451.
Cohen, M.C.L., Figueiredo, B.L., Oliveira, N.N., Fontes, N.A., França, M.C., Pessenda, L.C. R., Souza, A.V., Macario, K., Giannini, P.C.F., Bendassolli, J.A., Lima, P., 2020. Impacts of Holocene and modern sea-level changes on estuarine mangroves from northeastern Brazil. Ear. Surf. Process Landfor. 45, 375–392.
Colinvaux, P., De Oliveira, P.E., Patiño, J.E.M., 1999. Amazon Pollen Manual and Atlas. Harwood Acad. Publi, Dordrecht, p. 332.
Color, Munsell, 2009. Munsell Soil Color Charts, New, Revised edition. Macbeth Division of Kollmorgen Instruments, New Windsor, NY.
de Toniolo, T.F., Giannini, P.C.F., Angulo, R.J., de Souza, M.C., Pessenda, L.C.R., Spotorno-Oliveira, P., 2020. Sea-level fall and coastal water cooling during the late Holocene in Southeastern Brazil based on vermetid bioconstructions. Mar. Geol. 106281.
Deines, P., 1980. The isotopic composition of reduced organic carbon. In: Fritz, P., Fontes, J.Ch. (Eds.), Handbook of Env. Isto. Geoche., 1. The Terrestrial Environment. Elsevier, pp. 329–406.
Dominguez, J.M.L., 2009. The coastal zone of Brazil. In: Dillenburg, S.R., Hesp, P.A. (Eds.), Geology and Geomorphology of Holocene Coastal Barriers of Brazil. Springer Verlag, Berlin, pp. 17–51.
Dominguez, J.M., Bittencourt, A.C.S.P., Martin, L., 1981. Esquema evolutivo da sedimentação Quaternária nas feições deltaicas dos Rios São Francisco (SE/AL), Jequitinhonha (BA), Doce (ES) e Paraíba do Sul (RJ). São Paulo. Rev. Brasil. Geociên. 11 (4), 227–237.
Dominguez, J.L., Bittencourt, A.C.D.S.P., Martin, L., 1992. Controls on Quaternary coastal evolution of the east-northeastern coast of Brazil: roles of sea-level history, trade winds and climate. Sediment. Geol. 80 (3–4), 213–232.
Faegri, K., Inversen, J., 1989. Texbook of Pollen Analysis. John Wiley, New York, p. 486.
Fellerhoff, C., Voss, M., Wantzen, K.M., 2003. Stable carbon and nitrogen isotope signatures of decomposing tropical macrophytes. Aquat. Ecol. 37, 361–375.
Fernandes, G.W., Goulart, F.F., Ranieri, B.D., Coelho, M.S., Dales, K., Boesche, N., Bustamante, M., Carvalho, F.A., Carvalho, D.C., Dirzo, R., 2016. Deep into the mud: Ecological and socio-economic impacts of the dam breach in Mariana, Brazil. Nat. Conservação 14 (2), 35–45.
Fontes, N.A., Moraes, C.A., Cohen, M.C.L., Alves, I.C.C., França, M.C., Pessenda, L.C.R., Francisquini, M., Bendassolli, J.A., Macario, K., Mayle, F., 2017. The Impacts of the Middle Holocene High Sea-Level stand and Climatic changes on Mangroves of the Jucuruçu River, Southern Bahia - Northeastern Brazil. Radiocar. 59, 215–230.
França, M.C., Francisquini, M.I., Marcelo, C.L.C., Pessenda, L.C.R., Rosseti, D.F., Guimaraes, J.T.F., Smith, C.B., 2012. The last mangroves in Marajó Island – Eastern Amazon: climate and/or relative sea-level changes impacts. Rev. Palaeobot. Palynol. 187, 50–68.
França, M.C., Cohen, M.C.L., Pessenda, L.C.R., Rosseti, D.F., Lorente, F.L., Buso, A., Guimarães, J.T.F., Friaes, Y., 2013. Mangrove vegetation changes on Holocene terraces of the Doce River, southeastern Brazil. Catena (Cremlingen) 110, 59–69.
França, M.C., Francisquini, M.I., Cohen, M.C.L., Pessenda, L.C.R., 2014. Inter-proxy evidence for the development of the Amazonian mangroves during the Holocene. Veg. Hist. Archaeobotany 23, 527–542.
França, M.C., Alves, I.C.C., Castro, D.F., Cohen, M.C.L., Rossetti, D.F., Pessenda, L.C.R., Lorente, F.L., Fontes, N.A., Buso Jr., A.A., Giannini, P.C.F., da Francisquini, M.I., 2015. Multi-proxy evidence for the transition from estuarine mangroves to deltaic freshwater marshes, Southeastern Brazil, due to climatic and sea-level changes during the late Holocene. Catena 155–166.
França, M.C., Alves, I.C.C., Cohen, M.C.L., Rossetti, D.F., Pessenda, L.C.R., Giannini, P.C. F., Lorente, F.L., Buso Jr., A.A., Bendassolli, J.A., 2016. Millennial to secular time-scale impacts of climate and sea-levelchanges on mangroves from the Doce River Delta, Southeastern Brazil. Holocene 26, 1733–1749.
French, J.R., Stoddart, D.R., 1992. Hydrodynamics of salt marsh creek systems: Implications for marsh morphological development and material exchange. Earth Surf. Proc. Landfor. 17 (3), 235–252.
Furukawa, K., Wolanski, E., 1996. Sedimentation in mangrove forests. Mangrove Salt Marshes 1 (1), 3–10.
Gil-Torres, W., Ulloa-Delgado, G., 2001. Caracterización, Diagnóstico de los Manglares del Departamento de Córdoba Corporación Autónoma Regional de los Valles del Sinú y el San Jorge Montería, p. 195.

Grimm, E.C., 1987. CONISS: a Fortran 77 program for stratigraphically constrained cluster analysis by the method of incremental sum of squares. Comput. Geosci. 13, 13–35.
Grimm, E.C., 1990. TILIA and TILIAGRAPH: PC spreadsheet and graphic software for pollen data. In: INQUA Subcommission on Data-Handling Methods. Newsletter, 4, pp. 5–7.
Gu, X., Feng, H., Tang, T., Tam, N.F.Y., Pan, H., Zhu, Q., Dong, Y., Fazlioglu, F., Chen, L., 2019. Predicting the invasive potential of a non-native mangrove reforested plant (Laguncularia racemosa) in China. Ecol. Eng. 139, 105591.
Guimarães, J.T.F., Cohen, M.C.L., Pessenda, L.C.R., França, M.C., Smith, C.B., Nogueira, A.C.R., 2012. Mid- and Late-Holocene sedimentary process and palaeovegetation changes near the mouth of the Amazon River. Holocene 22, 359–370.
Harper, C.W., 1984. Improved methods of facies sequence analysis. In: Walker, R.G. (Ed.), Facies Models, 2nd ed. Geological Association of Canada, Ontario, Canada, pp. 11–13.
Hogarth, P.J., 2007. The Biology of Mangroves. Oxford University Press, New York (228p).
Hoguin, R., Restifo, F., 2012. Middle Holocene archaeology: dynamics of environmental and socio-cultural change in South America. Quat. Int. 256, 1–87.
Hutchings, P., Saenger, P., 1987. The Ecology of Mangroves. University of Queensland Press, Queensland.
Job, T., Penny, D., Morgan, B., Hua, Q., Gadd, P., Zawadzki, A., 2021. Multi-stage Holocene evolution of the River Murray Estuary, South Australia. Holocene 31 (1), 50–65.
Kathiresan, K., Thangam, T.S., 1990. A note on the effects of salinity and pH on growth of Rhizophora seedlings. Indian Forester 116 (3), 243–244.
Kirwan, M.L., Murray, A.B., 2007. A coupled geomorphic and ecological model of tidal marsh evolution. PNAS 104 (15), 6118–6122.
Krauss, K.W., McKee, K.L., Lovelock, C.E., Cahoon, D.R., Saintilan, N., Reef, R., Chen, L., 2013. How mangrove forests adjust to rising sea level. New Phytol. 202, 19–34.
Lamb, A.L., Wilson, G.P., Leng, M.J., 2006. A review of coastal palaeoclimate and relative sea level reconstructions using δ13C and C/N ratios in organic material. Earth-Sci. Rev. 75 (1), 29–57.
Lara, R.J., Cohen, M.C.L., 2009. Palaeolimnological studies and ancient maps confirm secular climate fluctuations in Amazonia. Clim. Chang. 94, 399–408.
Lorente, F.L., Pessenda, L.C.R., Oboh-Ikuenobe, F., Buso Junior, A.A., Cohen, M.C.L., Meyer, K.E.B., Giannini, P.C.F., Oliveira, P.E., Rossetti, D.F., Borotti Filho, M., França, M.C., Castro, D.F., Bendassolli, J.A., Macario, K., 2014. Palynofacies and stable C and N isotopes of Holocene sediments from Lake Macuco (Linhares, Espírito Santo, southeastern Brazil): Depositional settings and palaeoenvironmental evolution. Palaeogeogr. Palaeoclimatol. Palaeoecol. 415, 69–82.
Markgraf, V., D'Antoni, H.L., 1978. Pollen Flora of Argentina. University of Arizona Press, Tucson, AZ.
Martin, L., Suguio, K., 1992. Variation of coastal dynamics during the last 7000 years recorded in beach-ridge plains associated with river mouths: example from the central Brazilian coast. Palaeogeogr. Palaeoclimatol. Palaeoecol. 99, 119–140.
Martin, L., Bittencourt, A.C.S.P., Vilas Boas, G.S., Flexor, J.M., 1980. Mapa Geológico do Quaternário Costeiro do Estado da Bahia – 1:250.000: Texto Explicativo. Secretaria das Minas e Energia/coordenação da produção mineral, Salvador.
Martin, L., Suguio, K., Flexor, J.M., Dominguez, J.M.L., Bittencourt, A.C.S.P., 1996. Quaternary Sea-level history and variation in dynamics along the Central Brazil Coast: consequences on coastal plain construction. An. Acad. Bras. Cienc. 68, 303–354.
Martin, L., Dominguez, J.M.L., Bittencourt, A.C.S.P., 1998. Climatic control of coastal erosion during a sea-level fall episode. Ann. Acad. Bras. Ci. 70, 249–266.
Martin, L., Dominguez, J.M.L., Bittencourt, A.C.S.P., 2003. Fluctuating Holocene sealevels in eastern and southeastern Brazil: evidence from multiple fossil and geometric indicators. J. Coastal Res. Royal Palm Beach 19, 101–124.
Masselink, G., Gehrels, R., 2015. Coastal Environments & Global Change. Copyright © 2014. John Wiley & Sons, Ltd.
McKee, K.L., Cahoon, D.R., Feller, I.C., 2007. Caribbean mangroves adjust to rising sea level through biotic controls on change in soil elevation. Glob. Ecol. Biogeogr. 16 (5), 545–556.
Meyers, P.A., 2003. Applications of organic geochemistry to paleolimnological reconstructions: a summary of examples from the Laurentian Great Lakes. Org. Geochem. 34, 261–289.
Miall, A.D., 1978. Facies types and vertical profile models in braided river deposits: A summary. In: Miall, A.D. (Ed.), Fluvial Sedimentology. Canad. Soci. of Petrol. Geol, Calgary, pp. 597–604.
Milne, G.A., Bassett, E., 2005. Modeling Holocene relative sea-level observations from the caribbean and South America. Quat. Sci. Rev. 24 (10−11), 1183–1202.
Monacci, N.M., Meier-Gruenhagen, U., Finney, B.P., Behling, H., Wooller, M.J., 2009. Mangrove ecosystem changes during the Holocene at Spanish Lookout Cay, Belize. Palaeogeogr. Palaeoclimatol. Palaeoecol. 280, 37–46.
Naidoo, G., Hiralal, O., Naidoo, Y., 2011. Hypersalinity effects on leaf ultrastructure and physiology in the mangrove Avicennia marina. Flora-Morphol. Distrib. Funct. Ecol. Plants 206 (9), 814–820.
Peixoto, A.L., Gentry, A., 1990. Diversidade e composição florística da mata de tabuleiro na Reserva Florestal de Linhares (Espírito Santo, Brasil). Rev. Bras. Bot. 13, 19–25.
Pessenda, L.C.R., de Ribeiro, A.S., Gouveia, S.E.M., Aravena, R., Boulet, R., Bendassolil, J.A., 2004. Vegetation dynamics during the late Pleistocene in the Barreirinhas regions, Maranhão State, northeastan Brazil, based on carbon isotopes in soil organic matter. Quat. Res. 62, 183–193.
Pessenda, L.C.R., Gouveia, S.E.M., Ledru, M., Aravena, R., Ricardi-Branco, F.S., Bendassolli, J.A., de Ribeiro Adauto, S., Saia, S.E.M.G., Sifeddine, A., de Menor, E.A., de Oliveira, S.M.B., Cordeiro, R.C., de Freitas, A.M.M., Boulet, R., Filizola, H.F., 2008. Interdisciplinary paleovegetation study in the Fernando de Noronha Island (Pernambuco State), northeastern Brazil. Anais da Academia Brasileira de Ciências (Impresso) 80, 677–691.
Pessenda, L.C.R., Vidotto, E., De Oliveira, P.E., Buso Jr., A.A., Cohen, M.C.L., de Rossetti, D.F., Ricardi-Branco, F., Bendassol, J.A., 2012. Late Quaternary vegetation and coastal environmental changes at Ilha do Cardoso mangrove, southeastem Brazil. Palaeogeogr. Palaeoclimatol. Palaeoecol. 363-364, 57–68.
Peterson, B.J., Howarth, R.W., 1987. Sulfur, carbon, and nitrogen isotopes used to trace organic matter flow in the salt-marsh estuary of Sapelo Island, Georgia. Limnol. Oceanogr. 32, 1195–1213.
Reimer, P.J., Bard, E., Bayliss, A., Beck, J.W., Blackwell, P.G., Bronk, Ramsey C., 2013. Reimer, P. J. (Ed.) IntCal13 and marine13 radiocarbon age calibration curves 0–50,000 years cal BP. Radiocarbon 55 (4), 1869–1887.
Reineck, H.E., Singh, L.E., 1980. Depositional Sedimentary Environments. Springer-Verlag, Berlin, p. 551.
Rossetti, D.F., Ricardi-Branco, F., Bendassolli, J.A., 2012. Late Quaternary vegetation and coastal environmental changes at Ilha do Cardoso mangrove, southeastern Brazil. Palaeogeogr. Palaeoclimatol. Palaeoecol. 363, 57–68.
Rossetti, D.F., Bezerra, F.H., Dominguez, J.M.L., 2013. Late Oligocene-Miocene transgressions along the equatorial and eastern margins of Brazil. Earth-Sci. Rev. 123, 87–112.
Roubik, D.W., Moreno, J.E., 1991. Pollen and Spores of Barro Colorado. Missouri Botanical Garden, St. Louis, p. 270.
Salgado-Labouriau, M.L., 1973. Contribuição à Palinologia dos Cerrados. Academia Brasileira de Ciências, Rio de Janeiro, p. 273.
Smith, C.B., Cohen, M.C.L., Pessenda, L.C.R., França, M.C., Guimarães, J.T.F., de Rossetti, D.F., Lara, R.J., 2011. Holocene coastal vegetation changes at the mouth of the Amazon River. Rev. Palaeobot. Palynol. 168, 21–30.
Snedaker, S.C., 1982. Mangrove species zonation: Why? In: Sen, D.N., Rajpurohit, K.S. (Eds.), Contributions to the Ecology of Halophytes: Tasks for Vegetation Science, vol. 2. Springer, Netherlands, pp. 111–125.
Sobrado, M.A., 2000. Relation of water transport to leaf gas exchange properties in three mangrove species. Trees 14, 258–262.
Stuiver, M., Reimer, P.J., Reimer, R.W., 2018. CALIB 7.1 [WWW program]. http://calib.org (accessed 2019-5-27).
Suárez, N., Medina, E., 2005. Salinity effect on plant growth and leaf demography of the mangrove, Avicennia germinans L. Trees 19, 721–727.
Suguio, K., Martin, L., Flexor, J.M., 1980. Sea-level fluctuations during the past 6,000 years along the coast of the State of Silo Paulo, Brazil. In: Morncr, N.A. (Ed.), Earth Rheology, Isostasy and Eustasy. John Willey and Sons, pp. 471–486.
Suguio, K., Martin, L., Dominguez, J.M.L., 1982. Evolução da planície costeira de Rio Doce (ES) durante o Quaternário: influência das flutuações do nível do mar. In: Simpósio Do Quaternário Do Brasil, 4., 1982, Rio de Janeiro. Anais, Rio de Janeiro, pp. 93–116.
Sukigara, C., Saino, T., 2005. Temporal variations of $\delta^{13}C$ and $\delta^{15}N$ in organic particles collected by a sediment trap at timeseries station off the Tokyo Bay. Cont. Shelf Res. 25, 1749–1767.
Thom, B.G., 1984. Coastal landforms and geomorphic processes. In: Snedaker, S.C., Snedaker, J.C. (Eds.), The Mangrove Ecosystems: Research Methods. UNESCO, Bungay, UK, pp. 3–17.
Thomas, R.G., Smith, D.G., Wood, J.M., Visser, J., Calverley-Range, E.A., Koster, E.H., 1987. Inclined heterolithic stratification-terminology, description, interpretation andsignificance. Sediment. Geol. 53, 123–179.
Tognella, M.M.P., da Cunha, S.R., Soares, M.L.G., Schaeffer-Novelli, Y., Lugli, D.O., 2006. Mangrove evaluation - an essay. J. Coast. Res. 39, 1219–1224.
Tomlinson, P.B., 1986. The Botany of Mangroves. Cambridge University Press, USA, p. 413.
USEPA, 1999. Innovative Technology Verification Report: Sediment Sampling Technology, Aquatic Research Instruments Russian Peat Borer, EPA/600/R-01/010. Office of Research and Development.
Walker, R.G., James, N.P., 1992. Facies models and modern stratigrahic concepts. In: Walker, R.G., James, N.P. (Eds.), Facies Models - Response to Sea Level Change. Ontario, Canada, Geological Association of Canada, pp. 1–14.
Walker, M.J.C., Berkelhammer, M., Björck, S., Cwynar, L.C., Fisher, D.A., Long, A.J., Lowe, J.J., Newnham, R.M., Rasmussen, S.O., Weiss, H., 2012. Formal subdivision of the Holocene Series/Epoch: a Discussion Paper by a Working Group of INTIMATE (Integration of ice-core, marine and terrestrial records) and the Subcommission on Quaternary Stratigraphy (International Commission on Stratigraphy). J. Quat. Sci. 27, 649–659.
Wentworth, C.K., 1922. A scale of grade and class terms for clastic sediments. J. Geol. 30, 377–392.
Wilson, G.P., Lamb, A.L., Leng, M.J., Gonzalez, S., Huddart, D., 2005. Variability of organic δ13C and C/N in the Mersey Estuary, U.K. and its implications for sea-level reconstruction studies, Coastal and Shelf Science. London 64 (4), 685–698.
Wolanski, E., Mazda, Y., King, B., Gay, S., 1990. Dynamics, flushing and trapping in Hinchinbrook channel, a giant mangrove swamp, Australia. Estuar. Coast. Shelf Sci. 31 (5), 555–579.
Woodroffe, C.D., 1982. Geomorphology and development of Mangrove Swamps, Grand Cayman Island, West Indies. Bull. Mar. Sci. 32 (2), 381–398.
Woodroffe, C., 1992. Mangrove sediments and geomolphology. In: Robertson, Alongi (Eds.), Tropical Mangrove Ecosystems. AGU, Washington, pp. 7–41.
Woodroffe, C., 2002. Coasts: Form, Process, and Evolution. Cambridge University Press, New York.